THE JOURNAL OF PHYSICAL CHEMISTRY B

Article

pubs.acs.org/JPCB

Observing the Electrochemical Oxidation of Co Metal at the Solid/Liquid Interface Using Ambient Pressure X-ray Photoelectron Spectroscopy

Yong Han,[†,‡,⊥] Stephanus Axnanda,[§,⊥] Ethan J. Crumlin,[§] Rui Chang,[†] Baohua Mao,[†] Zahid Hussain,[§] Philip N. Ross,[∥] Yimin Li,[*,†,‡] and Zhi Liu[*,†,‡]

[†]State Key Laboratory of Functional Materials for Informatics, Shanghai Institute of Microsystem and Information Technology, Chinese Academy of Sciences, Shanghai 200050, People's Republic of China

[‡]School of Physical Science and Technology, Shanghai Tech University, Shanghai 200031, China

[§]Advanced Light Source, Lawrence Berkeley National Laboratory, Berkeley, California 94720, United States

[∥]Materials Sciences Division, Lawrence Berkeley National Laboratory, Berkeley, California 94720, United States

ABSTRACT: Recent advances of ambient pressure X-ray photoelectron spectroscopy (AP-XPS) have enabled the chemical composition and the electrical potential profile at a liquid/electrode interface under electrochemical reaction conditions to be directly probed. In this work, we apply this *operando* technique to study the surface chemical composition evolution on a Co metal electrode in 0.1 M KOH aqueous solution under various electrical biases. It is found that an ~12.2 nm-thick layer of $Co(OH)_2$ forms at a potential of about −0.4 $V_{Ag/AgCl}$, and upon increasing the anodic potential to about +0.4 $V_{Ag/AgCl}$, this layer is partially oxidized into cobalt oxyhydroxide (CoOOH). A CoOOH/$Co(OH)_2$ mixture layer is formed on the top of the electrode surface. Finally, the oxidized surface layer can be reduced to Co^0 at a cathodic potential of −1.35 $V_{Ag/Cl}$. These observations indicate that the ultrathin layer containing cobalt oxyhydroxide is the active phase for oxygen evolution reaction (OER) on a Co electrode in an alkaline electrolyte, consistent with previous studies.

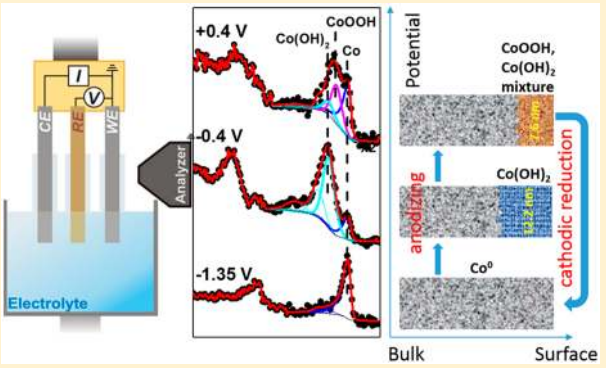

INTRODUCTION

The excessive use of fossil fuels has led to serious environmental problems, such as global warming. Direct water splitting to produce hydrogen and oxygen through electrochemical and photoelectrochemical processes is a promising renewable energy solution currently under intensive research and development.[1,2] The water splitting reaction consists of two half-cell reactions: the hydrogen evolution reaction (HER) at the cathodic half cell and the oxygen evolution reaction (OER) at the anodic half cell. The energy efficiency of electrochemical water-splitting is mainly limited by the OER process due to its high overpotential.[3,4] Extensive research effort has been made to develop the catalysts with low OER overpotentials. At present, Ir- and Ru-based compounds have the highest OER activities. However, the high cost of these precious metals prohibits their large scale commercial applications.[5] Among various earth abundant materials, cobalt-based catalysts have recently attracted wide attention owing to their relatively high catalytic activities for the OER.[5−9] A previous theoretical study suggests that CoOOH is the active phase where the OER occurs in alkaline media,[10] and using surface-enhanced Raman spectroscopy and X-ray absorption spectroscopy, several experimental studies indicate the formation of CoOOH on the Co-oxide catalysts under OER conditions.[2,11] However, key information such as the thickness and stability of the CoOOH layer is yet to be determined.

Recently, a new development of ambient pressure X-ray photoelectron spectroscopy (AP-XPS) has allowed the direct probing of the surface chemical composition, its depth profile, and electrical potential profile at a liquid/electrode interface under reaction conditions.[12−17] In previous studies, a "dip and pull" method was employed to create a stable nanometer-thick aqueous electrolyte on a platinum working electrode surface.[12] This ultrathin solid/liquid interface region was then probed *operando* during the electrochemical oxidation of the Pt electrode at an OER potential, and the formation of both Pt^{2+} and Pt^{4+} interfacial species was observed on the Pt foil surface. Recently, the OER reaction mechanism on a platinum electrode in an alkaline electrolyte was investigated by *operando* AP-XPS, and the $Pt^{\delta}-OH_{ads}$ was proposed to be the rate

Special Issue: Miquel B. Salmeron Festschrift

Received: June 18, 2017
Revised: August 24, 2017
Published: August 28, 2017

DOI: 10.1021/acs.jpcb.7b05982
J. Phys. Chem. B XXXX, XXX, XXX−XXX

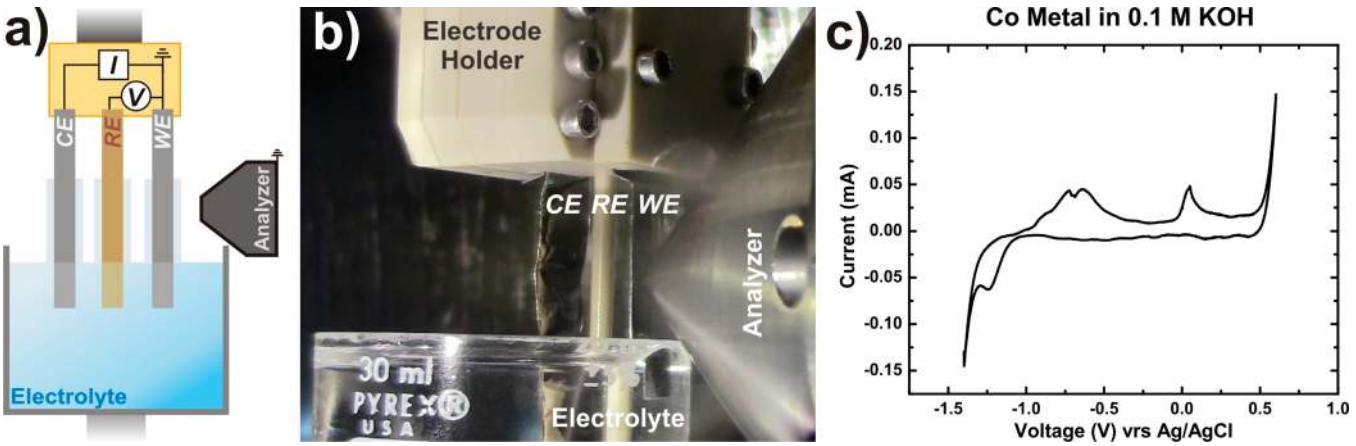

Figure 1. (a) Schematic diagram depicting the *operando* three-electrode system comprised of a platinum (Pt) metal foil counter electrode (CE), a silver/silver chloride (Ag/AgCl) reference electrode (RE), and a cobalt (Co) metal foil working electrode (WE). An electrochemically active solid/liquid interface is created by dipping into the solution and partially removing from an aqueous 0.1 M KOH electrolyte solution, referred to as the "dip and pull" method. (b) Photographic image of the experimental system, (c) Voltammogram of the dipped three-electrode setup into the electrolyte.

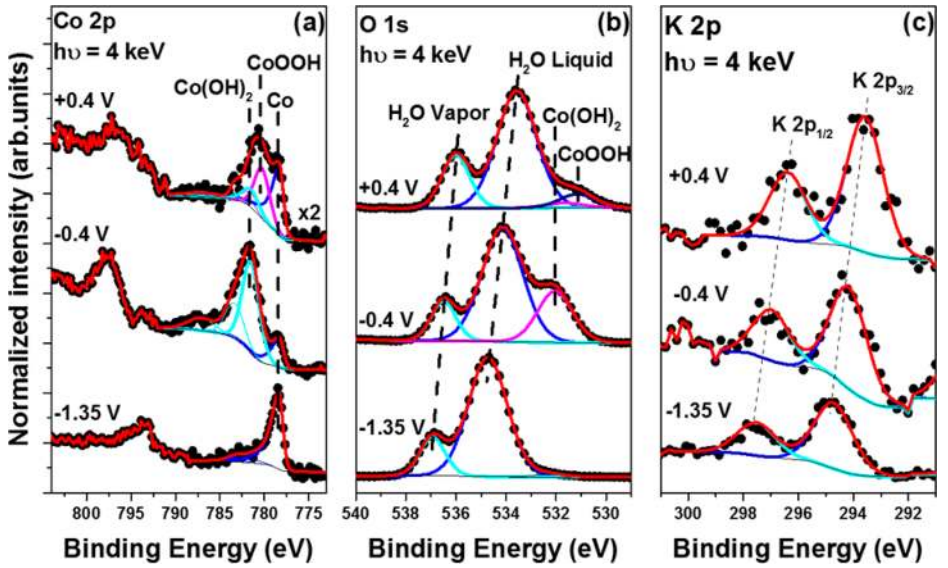

Figure 2. (a) Co 2p, (b) O 1s, and (c) K 2p spectra using the operando "dip and pull" method collected at −1.35, −0.4, and +0.4 V versus Ag/AgCl at $h\upsilon$ = 4 keV in 0.1 M KOH.

determining species for OER.[18] Investigations show the $Co_3O_4/Co(OH)_2$ biphasic electrocatalyst converts to CoOOH, which was determined to promote the enhanced electrocatalytic activity.[19] In this work, the same tender X-ray AP-XPS was used to characterize cobalt foil as the working electrode at different applied potentials in a 0.1 M KOH electrolyte. The evolution of the Co metal surface species was observed by acquiring Co 2p and O 1s spectra at various fixed potentials. By using Co foil as a simple model system, we used this surface sensitive technique (AP-XPS) to gain a fundamental understanding of the electrochemical oxidation of Co metal in a KOH electrolyte, which is an essential step for clarifying the catalysis mechanism and the active sites of the Co-base OER electrode.

EXPERIMENTAL SECTION

Following the previously reported experimental procedures,[12] the AP-XPS measurements were performed at bending magnet beamline 9.3.1 at the Advanced Light Source of the Lawrence Berkeley National Laboratory (Berkeley, USA). Beamline 9.3.1 provides X-rays in the "tender" energy range of 2.3−5.2 keV. The experiments were operated in a 20 Torr water vapor environment at room temperature (~20 °C). XPS spectra were mainly taken at a photon energy of 4.0 keV. At this photon energy, the photoelectron can penetrate through the thin liquid film created using a "dip and pull" method. The liquid film created using this method is continuous, electrically conductive, and typically ≲30 nm thick. Depth profiling was conducted by lowering the photon energy to $h\upsilon$ = 2.5 keV, which is more surface sensitive.

To probe the electrochemical solid/liquid interface properties of cobalt (Co) in 0.1 M KOH aqueous solution, as shown in Figure 1a and b, a Co metal foil working electrode (WE) was mounted in a three-electrode holder along with a silver/silver chloride (Ag/AgCl) reference electrode (RE) and a platinum (Pt) metal foil counter electrode (CE). Before mounting the Co WE, its surface was cleaned by mechanical scraping to remove any surface oxide layers. Upon immersing into the

DOI: 10.1021/acs.jpcb.7b05982
J. Phys. Chem. B XXXX, XXX, XXX−XXX

electrolyte, it was electrochemically cycled repeatedly between −1.4 and +0.6 V versus Ag/AgCl. All potentials expressed in this work are with respect to Ag/AgCl ($V_{Ag/AgCl}$) unless otherwise stated. Figure 1c shows a stable cyclic voltammogram. There are two oxidation peaks and one reduction peak at around −0.75, 0.10, and −1.25 V, respectively. The details of the electrochemical reactions on the Co electrode surface at these potentials are discussed below. After achieving a stable voltammogram, the experiments were conducted in different electrochemical conditions. Using the "dip and pull" method, the WE was partially pulled out from the electrolyte slowly, thus creating a stable and electrochemically continuous solid/liquid interface along the Co WE surface. The WE was grounded to the analyzer to ensure that any Co XPS peak binding energy (BE) shifts relative to the Co metal peak are associated with changes in chemical state. Hence, well-defined changes in the species within the electrolyte are induced with the applied potentials.

We simultaneously collect Co 2p (from the WE) and O 1s (from the liquid electrolyte); the electrode position is positioned such that both the aqueous electrolyte and the Co metal are detectable. By applying a small change of electrical potential, we can confirm that the electrolyte is electrically continuous through the detection of a rigid shift for the O 1s and K 2p electrolyte specific XPS peaks.[12] High resolution spectra of the Co 2p, O 1s, K 2p, and C 1s are then collected *operando* at −1.35, −0.4, and +0.4 V along the anodic cyclic voltammetry (CV) branch while the three electrodes are in contact with the electrolyte reservoir. All spectra are referenced to the metallic Co peak, which has a BE of 778.3 eV.[20]

RESULTS AND DISCUSSION

As shown in Figure 2a, the Co 2p spectrum shows a single metallic state by fitting of the Co $2p_{3/2}$ peak (at a cathodic potential of −1.35 V). Due to the plasmon loss peak contribution, three peaks located at BEs of 778.3, 781.3, and 783.3 eV are used in peak fitting. The Co metal spectrum is fitted by an asymmetric main peak at 778.3 eV and two plasmon loss peaks at 3.0 and 5.0 eV above the main peak, which belong to the surface plasmon and bulk plasmon peak, respectively.[20,21] In addition, the O 1s spectrum (Figure 2b) shows two main peaks at ∼535 and ∼537 eV, which are assigned to the aqueous electrolyte thin layer and the water vapor phase above the Co foil.[12,22] In Figure 2c, we show the K 2p signal originated from K ion in KOH electrolyte. The K 2p shows one single species (solvated K ion) and contains two main peaks due to the spin−orbit splitting (K $2p_{3/2}$ and K $2p_{1/2}$), with BEs at 294.7 and 297.5 eV, respectively.[12] The fact that we only observe Co metal is consistent with the calculated thermodynamic data provided in a Pourbaix diagram, which reveals the most stable species is metallic Co at −1.35 V applied potential in a pH 13 aqueous solution.[10] Hence, our first experimental result confirms the thermodynamic prediction that, at a holding potential of −1.35 V, the Co WE surface beneath the KOH solution is indeed metallic.

When the holding potential was changed to −0.4 V, new features on the high binding energy side of the metallic Co peaks appear (as shown in Figure 2a). The main peak is positioned at a BE of ∼781.5 eV. According to the XPS database on the National Institute of Standards and Technology (NIST) Web site, among most cobalt oxides and cobalt hydroxides, only the Co $2p_{3/2}$ BE of $Co(OH)_2$ lies above 781.0 eV.[23,24] Therefore, three additional peaks at BEs of 781.5, 783.3, and 787.1 eV (shown in cyan color) are used to fit the Co $2p_{3/2}$ spectrum. These three peaks come from the $Co(OH)_2$, demonstrating the formation of a cobalt hydroxide layer on the Co electrode upon voltage change.[21] In addition, a new peak in the O 1s spectrum at a BE of 532.0 eV (Figure 2b, shown in magenta color) also appears, further confirming the existence of $Co(OH)_2$.[25,26] Comparing the BE positions of the liquid phase from the thin film, one can find that both the O 1s and K 2p BEs shift to low BE as the holding potential changes from −1.35 to −0.4 V. This phenomenon, the rigid BE shift of liquid phase matches the electrochemical potential shift of the WE with respect to the Ag/AgCl RE, is described in detail in our previous study on a solid/liquid interface system by electrochemical oxidation of the Pt electrode.[12] Since the WE is grounded, the matching shifts between electrolyte BEs (O 1s and K 2p) and the potential change is direct evidence of the conductive nature of the thin electrolyte film. From the Pourbaix diagram, the oxidation of Co is expected in this voltage range. $Co(OH)_2$ is indeed the thermodynamically stable species at a potential of −0.4 V with respect to the Ag/AgCl RE (−0.18 V with respect to the standard hydrogen electrode, SHE).[10] The experimental results are once again in agreement with the thermodynamic calculations.

At −0.4 V holding potential, a $Co(OH)_2$ layer is formed on the Co electrode. Assuming a layer model of $Co(OH)_2$, we can calculate the $Co(OH)_2$ thickness using the ratio of oxidized Co signal to metallic Co signal

$$I_{Co(OH)_2}/I_{Co} = n_{Co(OH)_2}\cdot(1 - e^{-d/\lambda_{Co(OH)_2}})/(n_{Co}\cdot e^{-d/\lambda_{Co}}) \quad (1)$$

where $I_{Co(OH)_2}/I_{Co}$ is the ratio of the $Co(OH)_2$ signal to the metallic Co signal; $n_{Co(OH)_2}$ and n_{Co} are the atomic density in unit volume of $Co(OH)_2$ and Co; d is the thickness of the $Co(OH)_2$ layer; and λ is the inelastic mean free path (IMFP) of the photoelectron. The QUASES-IMFP-TPP2M ver. 3.0 software was used to estimate the IMFP, λ, in eq 1.[27] At 4 keV photon energy (3.32 keV for Co $2p_{3/2}$ photoelectron), $\lambda_{Co(OH)_2}$ and λ_{Co} were determined to be 5.8 and 3.9 nm, respectively. $I_{Co(OH)_2}/I_{Co}$ is 5.24 after the electrochemical oxidation. The $n_{Co(OH)_2}/n_{Co}$ is calculated to be 0.26, since $n = N_A\cdot\rho/M$. Hence, we estimate the thickness of the $Co(OH)_2$ film on WE to be ∼12.2 nm.

The appearance of $Co(OH)_2$ is also consistent with the CV results. From Figure 1c, there is an oxidation peak at −0.75 V. When taken with XPS data, the reaction shown in eq 2 begins to occur on the Co electrode surface at −0.75 V. Previously, Koza et al. made a similar observation and used this chemistry as a new method for preparation of $Co(OH)_2$ films by electrochemical deposition.[28]

$$Co + 2OH^- \rightarrow Co(OH)_2 + 2e^- \quad (2)$$

Further increasing the applied potential to +0.4 V, the Co surface and XPS spectrum evolve accordingly (shown in Figure 2a). As shown in Figure 1c, there is an oxidation peak at +0.05 V, indicating that the Co(II) is oxidized to a higher valence state. Previous electrochemical studies revealed that $Co(OH)_2$ is electrochemically oxidized to CoOOH in water-alkali electrolyzers in this voltage region.[2,28,29] Therefore, the formation of cobalt oxyhydroxide on the WE surface at +0.4 V holding potential is anticipated in our *operando* experiment. As shown in Figure 2a, there is an additional component which

DOI: 10.1021/acs.jpcb.7b05982
J. Phys. Chem. B XXXX, XXX, XXX−XXX

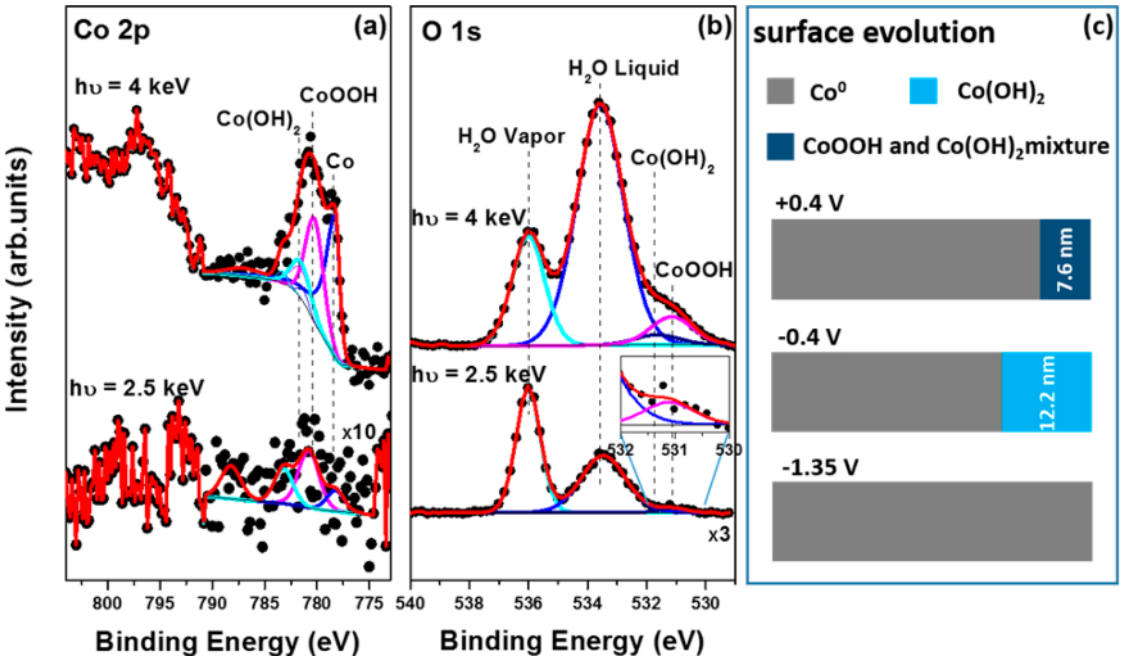

Figure 3. Depth profiling results. (a) Co 2p and (b) O 1s spectra at the photon energies of $h\upsilon$ = 4 and 2.5 keV during the *operando* "dip and pull" method collected at +0.4 $V_{Ag/AgCl}$ in 0.1 M KOH. (c) Schematic diagram depicting the evolution of the WE surface as a function of applied potential.

is located at a BE of ∼780.5 eV that appears in the Co 2p spectrum. According to the Pourbaix diagram,[10] Co_3O_4 and/or CoOOH are the most likely species that correspond to this new peak in the Co 2p spectrum at +0.4 V. The main peak BEs of Co_3O_4 and CoOOH are located at ∼779.5 and ∼780.3 eV, respectively.[19,21,24] We conclude that the new species formed at +0.4 V is CoOOH. Hence, three surface species are used to deconvolute the XPS spectrum. Beside Co and $Co(OH)_2$, another component exists in the spectrum. Two additional peaks at BEs of 780.3 and 781.6 eV (shown in magenta color) are needed. These two peaks are attributed to CoOOH.[19,24] Simultaneously, the appearance of a new peak (Figure 2b, shown in navy color) at a BE of 531.2 eV in the O 1s spectrum also shows the formation of cobalt oxyhydroxide at +0.4 V holding potential. Additional rigid BE shifts to low BEs of the O 1s and K 2p peaks of the liquid phase from the thin film (as shown in Figure 2b and c) are observed as the holding potential increases due to the additional potential added to the solid/liquid interface. In summary, the XPS results suggest that the further oxidation of the Co electrode when the applied potential is increased from −0.4 to +0.4 V. The surface of the $Co(OH)_2$ layer is partially converted into CoOOH, yet some $Co(OH)_2$ still remains.

Thermodynamically, CoOOH is the most stable species at +0.4 V potential with respect to the Ag/AgCl RE (+0.62 V with respect to SHE) for a Co electrode in 0.1 M KOH aqueous solution in the Pourbaix diagram.[10] However, the AP-XPS data demonstrate the formation of a mixed layer of CoOOH and $Co(OH)_2$ on the WE surface at this potential. Clearly, due to the kinetic limit, a single CoOOH phase is not observed. Nevertheless, we have identified the transformation to CoOOH at the pre-OER potential using AP-XPS and we believe that the ultrathin layer containing cobalt oxyhydroxide is the active phase for OER on a Co electrode in an alkaline electrolyte, as suggested by theory.[10]

The difference between the thermodynamic prediction and our experimental result is due to the kinetic limit. The conversion of $Co(OH)_2$ to CoOOH is believed to be a proton transfer process in the bulk that can be slow depending on the structure. This is a known phenomenon in the Ni electrode, the rate-limiting step of anodic oxidation of $Ni(OH)_2$ is the proton diffusion,[30−33] and both the kinetics and capacity (extent of conversion) depend on the structure of the $Ni(OH)_2$.[34] The Co alkaline cathode has not been studied to the same extent, but we believe the chemistry is the same. Hence, the rate-limiting step in the oxidation of $Co(OH)_2$ to CoOOH is a proton controlled process. In addition, α-$Ni(OH)_2$ is irreversibly transformed by dehydration into β-$Ni(OH)_2$ after the anodic oxidation of the Ni electrode to α-$Ni(OH)_2$ in an alkaline electrolyte. Moreover, the β-$Ni(OH)_2$ formed on the electrode cannot be reduced in successive cathodic sweeps.[35] An important finding of this work is that the anodic processes, unlike those on a Ni electrode, are completely reversible. The metallic state Co is easily restored following anodization. Since this study mainly focused on the investigation of surface chemical composition evolution of a Co electrode during electrochemical oxidation, the corresponding cathodic electrochemical processes will be further studied and discussed elsewhere.

The evolution of the surface layer of WE as a function of applied potential is summarized in Figure 3c. The cobalt WE surface is metallic at −1.35 V. It is converted into $Co(OH)_2$ at −0.4 V; Eventually, the Co WE is covered by a layer of CoOOH and $Co(OH)_2$ mixture at +0.4 V. Additionally, Koza et al. have found that the oxidation process of $Co(OH)_2$ to CoOOH is irreversible,[28] which is in agreement with our CV experiments. As shown in Figure 1c, there is no reduction peak corresponding to the oxidation peak at +0.05 V. The CoOOH is directly reduced to metallic Co at −1.25 V. Hence, the electrochemical reaction that occurs on the Co electrode surface at +0.05 V potential is described by eq 3.

$$Co(OH)_2 + OH^- \rightarrow CoOOH + H_2O + e^- \quad (3)$$

DOI: 10.1021/acs.jpcb.7b05982
J. Phys. Chem. B XXXX, XXX, XXX−XXX

To determine the spatial distributions of the chemical species, we performed depth profiling experiments on the cobalt electrode. By changing the photon energy from 4 to 2.5 keV, XPS probes a shallower region and is more surface sensitive. Several observations are made when we compare the Co 2p, O 1s, and K 2p spectra taken at +0.4 V at 4 keV photon energy to those taken at 2.5 keV (as shown in Figure 3). For Co 2p spectra (shown in Figure 3a), the main signal comes from oxidized Co, and the metallic Co signal is almost unobservable when probed at 2.5 keV. We attempted to do the peak fitting of this very noisy spectrum; three peaks at BEs of ∼778.3 eV (metallic Co), ∼780.5 eV (CoOOH), and ∼782.0 eV ($Co(OH)_2$) were used to fit the Co $2p_{3/2}$ spectrum. The intensity ratio of the metallic Co peak to the oxidized Co peaks is 0.17 at 2.5 keV photon energy, much less than that (0.76) observed at 4.0 keV photon energy. If the oxidized Co is formed under the metallic Co, or is evenly distributed in the metallic Co, this ratio at 2.5 keV photon energy should not be less than that observed at 4.0 keV photon energy. Hence, the cobalt (oxy)hydroxide mixture layer is formed on top of the Co metal electrode, not underneath the cobalt metal layer. However, the signal-to-noise ratio of the Co 2p spectrum is not sufficient to determine whether the remaining peak comes from CoOOH or $Co(OH)_2$. From the O 1s at $h\nu$ = 2.5 keV (shown in Figure 3b, bottom), a small peak at BE of 531.1 eV (the inset of Figure 3b) indicates the formation of a CoOOH layer under the thin electrolyte film. From the O 1s spectrum, we cannot positively identify the signal from $Co(OH)_2$ at 2.5 keV. Considering the surface sensitive nature at this photon energy, the depth profile results indicate that a mixture layer of CoOOH and $Co(OH)_2$ is formed on WE at +0.4 V and $Co(OH)_2$ on average is likely to be located below the CoOOH on the Co WE surface.

CONCLUSIONS

Combing the new AP-XPS endstation and the "dip and pull" method with a "tender" X-ray synchrotron radiation source (2−7 keV), we are able to investigate the electrochemical oxidation of a Co electrode in KOH aqueous electrolyte under *operando* conditions in a three-electrode system. The oxidation state of the Co WE responds to changes in applied potential. As the holding potential is altered from −1.35 to −0.4 V and further increased to +0.4 V, the Co metal WE surface is converted from metallic Co to $Co(OH)_2$, and finally oxidized to a CoOOH/$Co(OH)_2$ mixture. Therefore, the ultrathin oxide layer containing cobalt oxyhydroxide is believed to be the active phase for the oxygen evolution reaction (OER) on a Co electrode in KOH alkaline electrolyte. Although our experimental results are generally consistent with the thermodynamic prediction, the coexistence of $Co(OH)_2$ and CoOOH, a deviation from the Pourbaix diagram, highlights the importance of kinetic related factors at a working solid/liquid interface. Our results are in agreement with the previous theoretical study that suggested that CoOOH is the active phase when the OER takes place in alkaline media.[10]

AUTHOR INFORMATION

Corresponding Authors

*E-mail: liym1@shanghaitech.edu.cn.
*E-mail: zliu2@mail.sim.ac.cn.

ORCID

Ethan J. Crumlin: 0000-0003-3132-190X
Zhi Liu: 0000-0002-8973-6561

Author Contributions

⊥Y.H., S.A.: These authors contributed equally in this work.

Notes

The authors declare no competing financial interest.

ACKNOWLEDGMENTS

This work in China was supported by the National Natural Science Foundation of China (11227902) and the Science and Technology Commission of Shanghai Municipality (14520722100). Y.L. would like to acknowledge the support of the "Hundred Talents Program" of the Chinese Academy of Sciences. The Advanced Light Source was supported by the Director, Office of Science, Office of Basic Energy Sciences, of the U.S. Department of Energy under Contract No. DE-AC02-05CH11231.

REFERENCES

(1) Hunter, B. M.; Gray, H. B.; Muller, A. M. Earth-Abundant Heterogeneous Water Oxidation Catalysts. *Chem. Rev.* **2016**, *116*, 14120−14136.
(2) Subbaraman, R.; Tripkovic, D.; Chang, K.-C.; Strmcnik, D.; Paulikas, A. P.; Hirunsit, P.; Chan, M.; Greeley, J.; Stamenkovic, V.; Markovic, N. M. Trends in Activity for the Water Electrolyser Reactions on 3d M(Ni, Co, Fe, Mn) Hydr(oxy)oxide Catalysts. *Nat. Mater.* **2012**, *11*, 550−557.
(3) Walter, M. G.; Warren, E. L.; McKone, J. R.; Boettcher, S. W.; Mi, Q.; Santori, E. A.; Lewis, N. S. Solar Water Splitting Cells. *Chem. Rev.* **2010**, *110*, 6446−6473.
(4) Cook, T. R.; Dogutan, D. K.; Reece, S. Y.; Surendranath, Y.; Teets, T. S.; Nocera, D. G. Solar Energy Supply and Storage for the Legacy and Non Legacy Worlds. *Chem. Rev.* **2010**, *110*, 6474−6502.
(5) Wang, J.; Cui, W.; Liu, Q.; Xing, Z.; Asiri, A. M.; Sun, X. Recent Progress in Cobalt-Based Heterogeneous Catalysts for Electrochemical Water Splitting. *Adv. Mater.* **2016**, *28*, 215−230.
(6) Cheng, F.; Shen, J.; Peng, B.; Pan, Y.; Tao, Z.; Chen, J. Rapid Room-Temperature Synthesis of Nanocrystalline Spinels as Oxygen Reduction and Evolution Electrocatalysts. *Nat. Chem.* **2011**, *3*, 79−84.
(7) Rosen, J.; Hutchings, G. S.; Jiao, F. Ordered Mesoporous Cobalt Oxide as Highly Efficient Oxygen Evolution Catalyst. *J. Am. Chem. Soc.* **2013**, *135*, 4516−4521.
(8) Wang, H.-Y.; Hung, S.-F.; Chen, H.-Y.; Chan, T.-S.; Chen, H. M.; Liu, B. In Operando Identification of Geometrical-Site-Dependent Water Oxidation Activity of Spinel Co_3O_4. *J. Am. Chem. Soc.* **2016**, *138*, 36−39.
(9) Xu, L.; Jiang, Q.; Xiao, Z.; Li, X.; Huo, J.; Wang, S.; Dai, L. Plasma-Engraved Co_3O_4 Nanosheets with Oxygen Vacancies and High Surface Area for the Oxygen Evolution Reaction. *Angew. Chem., Int. Ed.* **2016**, *55*, 5277−5281.
(10) Bajdich, M.; Garcia-Mota, M.; Vojvodic, A.; Norskov, J. K.; Bell, A. T. Theoretical Investigation of the Activity of Cobalt Oxides for the Electrochemical Oxidation of Water. *J. Am. Chem. Soc.* **2013**, *135*, 13521−13530.
(11) Yeo, B. S.; Bell, A. T. Enhanced Activity of Gold-Supported Cobalt Oxide for the Electrochemical Evolution of Oxygen. *J. Am. Chem. Soc.* **2011**, *133*, 5587−5593.
(12) Axnanda, S.; Crumlin, E. J.; Mao, B. H.; Rani, S.; Chang, R.; Karlsson, P. G.; Edwards, M. O. M.; Lundqvist, M.; Moberg, R.; Ross, P.; et al. Using "Tender" X-ray Ambient Pressure X-ray Photoelectron Spectroscopy as a Direct Probe of Solid-Liquid Interface. *Sci. Rep.* **2015**, *5*, 9788.
(13) Masuda, T.; Yoshikawa, H.; Noguchi, H.; Kawasaki, T.; Kobata, M.; Kobayashi, K.; Uosaki, K. In Situ X-ray Photoelectron Spectroscopy for Electrochemical Reactions in Ordinary Solvents. *Appl. Phys. Lett.* **2013**, *103*, 111605.

DOI: 10.1021/acs.jpcb.7b05982
J. Phys. Chem. B XXXX, XXX, XXX−XXX

(14) Lichterman, M. F.; Hu, S.; Richter, M. H.; Crumlin, E. J.; Axnanda, S.; Favaro, M.; Drisdell, W.; Hussain, Z.; Mayer, T.; Brunschwig, B. S.; et al. Direct Observation of the Energetics at a Semiconductor/Liquid Junction by Operando X-ray Photoelectron Spectroscopy. *Energy Environ. Sci.* **2015**, *8*, 2409−2416.
(15) Ali-Löytty, H.; Louie, M. W.; Singh, M. R.; Li, L.; Casalongue, H. G. S.; Ogasawara, H.; Crumlin, E. J.; Liu, Z.; Bell, A. T.; Nilsson, A.; et al. Ambient-Pressure XPS Study of a Ni-Fe Electrocatalyst for the Oxygen Evolution Reaction. *J. Phys. Chem. C* **2016**, *120*, 2247−2253.
(16) Brown, M. A.; Redondo, A. B.; Sterrer, M.; Winter, B.; Pacchioni, G.; Abbas, Z.; van Bokhoven, J. A. Measure of Surface Potential at the Aqueous-Oxide Nanoparticle Interface by XPS from a Liquid Microjet. *Nano Lett.* **2013**, *13*, 5403−5407.
(17) Favaro, M.; Jeong, B.; Ross, P. N.; Yano, J.; Hussain, Z.; Liu, Z.; Crumlin, E. J. Unravelling the Electrochemical Double Layer by Direct Probing of the Solid/Liquid Interface. *Nat. Commun.* **2016**, *7*, 12695.
(18) Favaro, M.; Valero-Vidal, C.; Eichhorn, J.; Toma, F. M.; Ross, P. N.; Yano, J.; Liu, Z.; Crumlin, E. J. Elucidating the Alkaline Oxygen Evolution Reaction Mechanism on Platinum. *J. Mater. Chem. A* **2017**, *5*, 11634−11643.
(19) Favaro, M.; Yang, J. H.; Nappini, S.; Magnano, E.; Toma, F. M.; Crumlin, E. J.; Yano, J.; Sharp, I. D. Understanding the Oxygen Eveolution Reaction Mechanisms on CoO_x using Operando Ambient Pressure X-ray Photoelectron Spectroscopy. *J. Am. Chem. Soc.* **2017**, *139*, 8960−8970.
(20) Powell, C. J. Recommended Auger Parameters for 42 Elemental Solids. *J. Electron Spectrosc. Relat. Phenom.* **2012**, *185*, 1−3.
(21) Biesinger, M. C.; Payne, B. P.; Grosvenor, A. P.; Lau, L. W. M.; Gerson, A. R.; Smart, R. S. C. Resolving Surface Chemical States in XPS Analysis of First Row Transition Metals, Oxides and Hydroxides: Cr, Mn, Fe, Co and Ni. *Appl. Surf. Sci.* **2011**, *257*, 2717−2730.
(22) Yamamoto, S.; Bluhm, H.; Andersson, K.; Ketteler, G.; Ogasawara, H.; Salmeron, M.; Nilsson, A. In Situ X-ray Photoelectron Spectroscopy Studies of Water on Metals and Oxides at Ambient Conditions. *J. Phys.: Condens. Matter* **2008**, *20*, 184025.
(23) Tan, B. J.; Klabunde, K. J.; Sherwood, P. M. A. XPS Studies of Solvated Metal Atom Dispersed (SMAD) Catalysts. Evidence for Layered Cobalt-Manganese Particles on Alumina and Silica. *J. Am. Chem. Soc.* **1991**, *113*, 855−861.
(24) Mattogno, G.; Ferragina, C.; Massucci, M. A.; Patrono, P.; Laginestra, A. X-ray Photoelectron Spectroscopic Evidence of Interlayer Complex Formation between Co(II) and N-Heterocycles in α-$Zr(HPO_4)_2 \cdot H_2O$. *J. Electron Spectrosc. Relat. Phenom.* **1988**, *46*, 285−295.
(25) McIntyre, N. S.; Cook, M. G. X-ray Photoelectron Studies on Some Oxides and Hydroxides of Cobalt, Nickel, and Copper. *Anal. Chem.* **1975**, *47*, 2208−2213.
(26) Yang, J.; Liu, H.; Martens, W. N.; Frost, R. L. Synthesis and Characterization of Cobalt Hydroxide, Cobalt Oxyhydroxide, and Cobalt Oxide Nanodiscs. *J. Phys. Chem. C* **2010**, *114*, 111−119.
(27) QUASES-IMFP-TPP2M Inelastic electron mean free path calculated from the Tanuma, Powell, and Penn TPP2M formula in Tanuma, S.; Powell, C. J.; Penn, D. R. *Surf. Interface Anal.* **1994**, *21*, 165−176, 10.1002/sia.740210302. Code written by Sven Tougaard. Copyright 2000−2010 Quases-Tougaard Inc. Free to use for non-commercial applications.
(28) Koza, J. A.; Hull, C. M.; Liu, Y.-C.; Switzer, J. A. Deposition of β-$Co(OH)_2$ Films by Electrochemical Reduction of Tris-(ethylenediamine)Cobalt(III) in Alkaline Solution. *Chem. Mater.* **2013**, *25*, 1922−1926.
(29) Liu, Y.-C.; Koza, J. A.; Switzer, J. A. Conversion of Electrodeposited $Co(OH)_2$ to CoOOH and Co_3O_4, and Comparison of Their Catalytic Activity for the Oxygen Evolution Reaction. *Electrochim. Acta* **2014**, *140*, 359−365.
(30) Macarthur, D. M. The Hydrated Nickel Hydroxide Electrode Potential Sweep Experiments. *J. Electrochem. Soc.* **1970**, *117*, 422.
(31) Weidner, J. W.; Timmerman, P. Effect of Proton Diffusion, Electron Conductivity, and Charge-Transfer Resistance on Nickel Hydroxide Discharge Curves. *J. Electrochem. Soc.* **1994**, *141*, 346−351.
(32) Paxton, B.; Newman, J. Variable Diffusivity in Intercalation Materials: A Theoretical Approach. *J. Electrochem. Soc.* **1996**, *143*, 1287−1292.
(33) Motupally, S.; Streinz, C. C.; Weidner, J. W. Proton Diffusion in Nickel Hydroxide-Prediction of Active Material Utilization. *J. Electrochem. Soc.* **1998**, *145*, 29−34.
(34) Seghiouer, A.; Chevalet, J.; Barhoun, A.; Lantelme, F. Electrochemical Oxidation of Nickel in Alkaline Solutions: A Voltammetric Study and Modelling. *J. Electrochem. Soc.* **1998**, *442*, 113−123.
(35) Medway, S. L.; Lucas, C. A.; Kowal, A.; Nichols, R. J.; Johnson, D. In Situ Studies of the Oxidation of Nickel Electrodes in Alkaline Solution. *J. Electrochem. Soc.* **2006**, *587*, 172−181.

DOI: 10.1021/acs.jpcb.7b05982
J. Phys. Chem. B XXXX, XXX, XXX−XXX